Fast B1 mapping with EPI

E. De Vita[1], D. L. Thomas[1], R. Deichmann[2], R. Turner[1], R. J. Ordidge[1]

[1]Wellcome Trust High Field MR Research Laboratory, Department of Medical Physics and Bioengineering, University College London, London, United Kingdom,
[2]Wellcome Department of Imaging Neuroscience, Institute of Neurology, University College London, London, United Kingdom

Introduction Non-uniformity of the rf excitation/reception field (B1) is a well known source of problems in many MR applications. The B1 distribution is affected by both intrinsic rf coil field profile in-vacuum and interactions between the B1 field, the sample (e.g. subject) and the coil. At high magnetic fields and for whole body applications these interactions are exacerbated by the fact that the rf wavelength in tissue becomes comparable to the sample and coil dimensions. In conventional MR techniques, the strong ensuing B1 inhomogeneity leads to problems such as unacceptably variable image contrast, cortical segmentation difficulties and unreliable parameter estimation. The design of MR methods with reduced B1 sensitivity benefits enormously from an accurate knowledge of the B1 distribution in the actual sample/subject under investigation. Whilst many B1 mapping methods have been proposed [1], they are limited by poor volume coverage per unit time and often the need for region of interest (roi) based analysis [2, 3]. Here, a method based on EPI is presented allowing the B1 distribution to be reliably and quickly obtained in-vivo. The method was applied successfully at 4.7T on phantoms and in-vivo and may constitute an extremely useful tool for quantitative MR and the development of methods that are less sensitive to B1 variations.

Theory & Methods Our B1 mapping method employs a hard pulse of constant amplitude and variable length (Tp) applied before a spoiler gradient. This leaves a longitudinal magnetisation ideally given by $Mz(\mathbf{r},Tp)=M_0(r)\cos(2\pi\nu_1(\mathbf{r})Tp)$ [Eq. 1] where $\mathbf{r}$ indicates spatial position, $M_0(\mathbf{r})$the equilibrium magnetisation and $\nu_1=\gamma B1/2\pi$ the precession frequency associated with the rf field B1 (with γ the gyromagnetic ratio). An EPI sequence is used to form images of Mz($\mathbf{r}$,Tp) for a number of Tp values (as suggested in [4]). Whilst the cosinusoidal expression in Eq. 1 would allow for a straightforward extraction of $\nu_1(r)$ (the B1 map) from such data sets, relaxation during and after the hard pulse (especially for multi-slice acquisitions) and off-resonance effects complicate the data analysis. For example, in off-resonance conditions, Eq. 1 becomes: $Mz(\mathbf{r},Tp)=M_0(r)\ (\sin^2\beta(\mathbf{r})\cdot\cos(2\pi\nu_{eff}(\mathbf{r})Tp)+\cos^2\beta(\mathbf{r}))$ [Eq. 2] where $\beta(\mathbf{r})$ is the angle between the effective field $\mathbf{B_{eff}=\Delta B0+B1}$, and the B0 axis, $\nu_{eff}=\gamma B_{eff}/2\pi$ and $\Delta B0=\Delta\omega/\gamma$ is the field offset associated with the resonance offset ($\Delta\omega$). For an acquisition where multiple slices are acquired in succession following the hard pulse preparation, longitudinal relaxation occurs in the interval (td) between preparation period and slice excitation; Eq. 1 becomes (in on-resonance conditions): $Mz(\mathbf{r},Tp,td)=M_0(\mathbf{r})\cos(2\pi\nu_1(\mathbf{r})Tp)e^{-td/T1(r)}+M_0(\mathbf{r})(1-e^{-td/T1(r)})$ [Eq. 3], thus acquiring a tissue dependence (associated to T1). These expressions show that oscillation frequency, maxima and zero-crossings are modified and these parameters become unreliable for estimating a B1 map. A point-by-point non-linear fit becomes awkward due to the number of parameters that need to be incorporated in the equations and convergence to meaningful parameter estimates is not assured. We have developed a data analysis method based on the Fourier Transform (FT) that is robust to relaxation effects even for multi-slice acquisition and short repetition times (TR) and is amenable to a quick and automated implementation. If images of Mz($\mathbf{r}$,Tp) for enough values of Tp have been collected, an FT of the corresponding images can be performed along the Tp dimension. The position of the maximum frequency in the spectrum associated with each pixel corresponds to the dominant frequency at the corresponding position (i.e. $\nu_{eff}(\mathbf{r})$) and allows a B_{eff} map to be obtained. Whilst the intrinsic resolution of the B_{eff} map is given by 1/Max(Tp), such resolution can be improved by zero-filling the data along the Tp direction prior to the FT. In typical conditions the difference between B1 and B_{eff} maps is small (e.g. 7.7% at 4.7T for ν_1=500Hz and $\Delta B0$=1ppm); this difference can be reduced by increasing the amplitude of the preparation pulse or accurately corrected using an acquired B0 map. A snapshot image showing iso-B1 (i.e. iso-B_{eff}) contours can also be obtained using a long Tp (such that $\nu_1(\mathbf{r})Tp$ corresponds to several full revolutions) followed by an EPI acquisition (as done with FLASH in [5]). Such an image can be extremely useful for determining the rough B1 distribution and the location of rf 'hot-spots'.

Materials & Results Imaging was performed on a 4.7T whole body scanner (provided by Philips, based on a SMIS design) with a standard quadrature birdcage head coil (16 rungs, Ø=28cm, length=20.9cm). A spin echo (SE) EPI sequence was used with *TR/TE*=2s/18ms; data matrix was 100x64 (sinusoidal read gradients) interpolated to 64x64. For the preparation pulse, the B1 amplitude was typically adjusted to have a nominal B1 over the calibration slice corresponding to ν_1=500Hz (i.e. 500µs for a 90º pulse). Typically, Tp was incremented from 0 to 5ms in 0.1ms intervals (δtp). The 50 data points were zero-filled to 512 to yield a B1 field resolution of 1/(δtp·512)=19.5Hz. Phantoms and consenting healthy human volunteers were scanned with the protocol detailed above and the data processed with the FT based method. Fig. 1-2 show B1 (B_{eff}) maps (axial, coronal, sagittal) of a spherical oil phantom (diameter 20cm) and a human head. The B1 distribution in the oil phantom is consistent with the one expected for a birdcage coil (saddle shaped in the coronal/sagittal views and dome-shaped in the axial view). In the human head, sample/rf/coil interactions produce a remarkable rf focusing in the center of the head (with a hot-spot at the level of the body of the corpus callosum) consistent with previous observations [6].

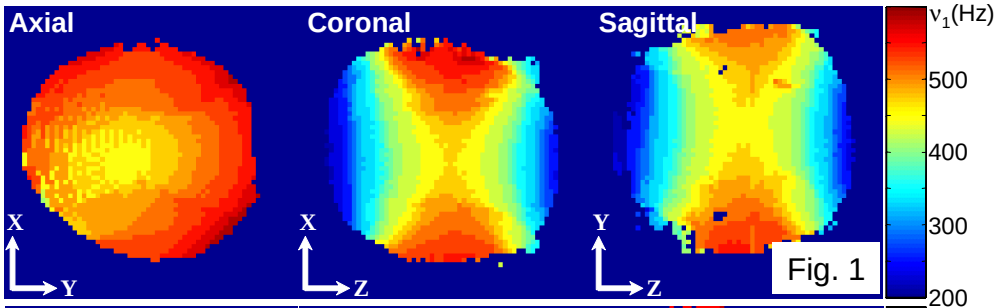

Fig. 1

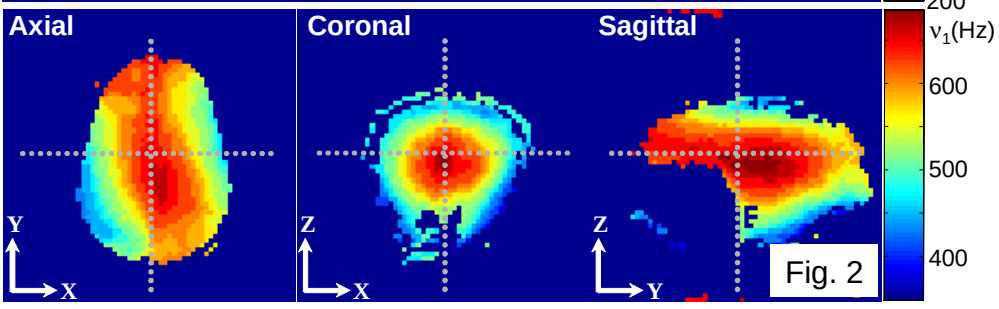

Fig. 2

Discussion & Conclusion The acquisition and data processing strategies presented constitute a quick and robust method of obtaining B1 maps in-vivo. The method could be extremely useful at high static magnetic fields (where B_1 inhomogeneities are exacerbated) in order to devise and assess the performance of MR sequences that have a reduced B1 sensitivity or post-acquisition correction technique.

Acknowledgments We thank the Wellcome Trust for financial support of this project. **References:** (1) References in Table 2.1 in *Quantitative MRI of the Brain: Measuring Changes Caused by Disease*, Tofts P editor, John Wiley & Sons, 2003. (2) Barker G *et al.*, BJR 71:59-67 (1998). (3) Vaughan *et al.*, MRM 46: 24-30 (2001). (4) Topp S *et al.*, Proc. 5th ISMRM, p281 (1997). (5) Deichmann R *et al.*, MRM 47: 398-402 (2002). (6) Barfuss H et al., Radiology 169:811-816 (1988). **Fig. 1** B1 maps of a spherical oil phantom. (Ø=20cm). Field of view (FoV) is 240mm and slice thickness 3mm. **Fig. 2** B1 maps of a human head. Dotted lines indicate the position of the orthogonal views. FoV=229mm, slice thickness=4mm. NB: the figures display B_{eff} maps rather than B1 maps as no B0 correction was performed.